

# Association of deletions and translocation of the reduced folate carrier gene with profound loss of gene expression in methotrexate-resistant K562 human erythroleukemia cells

Bee Ching Ding<sup>a</sup>, Teah L. Witt<sup>b</sup>, Bharati Hukku<sup>c</sup>, Henry Heng<sup>d</sup>, Long Zhang<sup>b</sup>,  
Larry H. Matherly<sup>a,b,\*</sup>

<sup>a</sup>Department of Pharmacology, Wayne State University School of Medicine, Detroit, MI 48201, USA

<sup>b</sup>Experimental and Clinical Therapeutics Program, Barbara Ann Karmanos Cancer Institute, Wayne State University School of Medicine, 110 East Warren Ave., Detroit, MI 48201, USA

<sup>c</sup>Cell Culture Laboratory, Children's Hospital of Michigan, Detroit, MI 48201, USA

<sup>d</sup>Center of Molecular Medicine and Genetics, Wayne State University School of Medicine, Detroit, MI 48201, USA

Received 24 May 2000; accepted 11 August 2000

## Abstract

Severe impairment of methotrexate membrane transport in methotrexate-resistant K562 (K500E) cells was characterized by a nearly complete loss of reduced folate carrier (RFC) transcripts and RFC protein. As determined by 5'-rapid amplification of cDNA ends (5'-RACE), ~93% of the RFC transcripts in wild-type cells contained the KS43 5'-untranslated region transcribed from the RFC-B promoter. KS43 transcripts decreased > 90% in K500E cells. The basal and full-length RFC-B promoters were more active (3- and 2-fold, respectively) in directing transcription of a luciferase reporter gene in K500E than in wild-type cells. Treatment with a demethylating agent, 5-aza-2'-deoxycytidine, or with a histone deacetylase inhibitor, trichostatin A, did not increase the levels of RFC transcripts in K500E cells. No differences in RFC gene structure were detected between the lines on Southern blots; however, the RFC signals were decreased approximately 60% in K500E cells. DNA sequences were identical between the lines for the RFC coding region and the two 5'-non-coding exons and their respective promoters. Spectral karyotype analysis and fluorescence *in situ* hybridization in wild-type cells showed two normal chromosome 21 copies and one or two marker chromosomes, each with an RFC signal. In K500E cells, the RFC gene locus was no longer localized to a normal chromosome 21 (at 21q22.2), and a single RFC signal was associated with a small metacentric chromosome, characterized by a 21/22 translocation. Our results suggest that loss of RFC transcripts in K500E cells is unrelated to changes in the levels of critical transcription factors, or to differences in the extent of RFC promoter methylation or core histone deacetylation. Rather, this phenotype is due to the loss of one or more RFC alleles, and to a translocation of the remaining RFC allele with the formation of a 21/22 fusion chromosome. © 2001 Elsevier Science Inc. All rights reserved.

**Keywords:** Chromosome 21; Membrane transport; Methotrexate; Reduced folate carrier; Resistance

## 1. Introduction

MTX continues to play an important role in the chemotherapy of human malignancies including acute lymphoblas-

tic leukemia, lymphoma, osteosarcoma, breast cancer, and head and neck cancer [1]. In general, MTX antitumor activity correlates with transport efficiency and results from the generation of high intracellular levels of unbound MTX for maximal DHFR inhibition and polyglutamylation catalyzed by FPGS [2, 3]. Further, incomplete inhibition of DHFR, due to impaired MTX transport, is a major mechanism of MTX resistance *in vitro* [2–4] and *in vivo* [5], and likely contributes to variations in clinical response, as well [6, 7].

Impaired MTX uptake results from reduced rates of carrier translocation, decreased transport substrate binding, or a composite of these effects. With the cloning of cDNAs for rodent [8, 9] and human [10–13] RFCs, a number of laboratories have begun to characterize the underlying bases for defective MTX uptake accompanying MTX resistance. It has been reported that the loss of MTX uptake capacity

\* Corresponding author. Tel.: +1-313-833-0715, Ext. 2407; fax: +1-313-832-7294.

E-mail address: matherly@kci.wayne.edu (L.H. Matherly).

**Abbreviations:** MTX, methotrexate; DAPI, 4',6-diamidino-2-phenylindole; 5'-UTRs, 5'-untranslated regions; 5'-RACE, 5'-rapid amplification of cDNA ends; DHFR, dihydrofolate reductase; FISH, fluorescence *in situ* hybridization; FPGS, folypolyglutamate synthetase; GST, glutathione-S-transferase; hRFC, human reduced folate carrier; mRFC, murine reduced folate carrier; APA-<sup>125</sup>I-ASA-Lys, N<sup>ε</sup>-(4-amino-4-deoxy-10-methylpteroyl)-N<sup>ε</sup>-(4-azido-5-<sup>125</sup>I-salicylyl)-L-lysine; ORF, open reading frame; PCR, polymerase chain reaction; PVDF, polyvinylidene difluoride; RFC, reduced folate carrier; RT-PCR, reverse transcription-polymerase chain reaction; and SKY, spectral karyotype.

for the mRFC is caused by a mutation in the RFC protein where proline-130 is replaced by alanine [14]. A G to A transition at position 890 of mRFC resulted in a substitution of serine-297 by asparagine and a selective decrease in MTX binding affinity (~4-fold) without effects on other antifolate analogs (aminopterin, 10-ethyl-10-deazaaminopterin; [15]). Similarly, replacement of serine-46 by asparagine in mRFC [16] or of glutamate-45 by lysine in both mRFC [17] and hRFC [18] resulted in greater impairment of uptake for MTX than (6S)-5-formyl tetrahydrofolate. In still other reports, losses of full-size RFC protein were described in spite of seemingly normal levels of RFC transcripts [19–21]. In these cases, RFC protein was undetectable due to early translation termination (resulting from frame shift mutations; [19–21]) and/or to accelerated rates of turnover of a mutant RFC protein [20, 21]. Whereas “transcriptionally silent” wild-type RFC alleles in drug-resistant sublines have been described in several reports [14, 20–23], the underlying mechanism(s) remains largely uncharacterized.

In this study, we examined the molecular bases for the nearly complete loss of hRFC transcripts and protein in transport-impaired K562 human erythroleukemia cells (designated K500E) selected for high levels of MTX resistance [22]. Our results suggest that the decreased hRFC transcripts are not related to changes in the levels of critical transcription factors, or to differences in hRFC promoter methylation or core histone deacetylation. Rather, the K500E phenotype is primarily the result of a loss of one or more hRFC alleles, and a translocation of the remaining hRFC allele with the formation of a t(21; 22) fusion chromosome.

## 2. Materials and methods

### 2.1. Materials

[ $\alpha$ - $^{32}$ P]dCTP (3000 Ci/mmol) and [ $\alpha$ - $^{35}$ S-thiol]dATP (1400 Ci/mmol) were obtained from Du-Pont/New England Nuclear. [3', 5', 7- $^3$ H]MTX (20 Ci/mmol) was purchased from Moravsek Biochemicals. Unlabeled MTX was provided by the Drug Development Branch, National Cancer Institute. Both labeled and unlabeled MTX were purified by HPLC prior to use [24]. Sequenase (version 2.0) and reagents for dideoxynucleotide sequencing were obtained from the United States Biochemical Corp. Restriction and modifying enzymes were purchased from Promega. Synthetic oligonucleotides were obtained from Genosys Biotechnologies, Inc. or Life Technologies.

### 2.2. Cell culture

The wild-type K562 erythroleukemia line was obtained from the American Type Culture Collection. Cells were maintained in RPMI 1640 containing 10% heat-inactivated iron-supplemented calf serum (Hyclone Laboratories), 2 mM l-glutamine, 100 U/mL of penicillin, and 100  $\mu$ g/mL of

streptomycin, in a humidified atmosphere at 37° in the presence of 5% CO<sub>2</sub>/95% air. The transport-impaired K500E subline was selected from wild-type K562 cells by soft agar cloning in the presence of 500 nM MTX as previously described [22]. K500E cells were maintained continuously in the presence of 500 nM MTX. Before assay of [ $^3$ H]MTX transport, cells were cultured for at least three generations without MTX. Cell lines were subcultured every 96 hr. Cell numbers were determined by direct microscopic counting with a hemacytometer.

### 2.3. [ $^3$ H]Mtx transport assays

Initial uptake of [ $^3$ H]MTX was assayed over 180 sec using  $1 \times 10^7$  cells/mL and an MTX concentration of 0.5  $\mu$ M [10, 22]. The levels of intracellular radioactivity were expressed as picomoles per milligram of protein, calculated from direct measurements of radioactivity and protein contents of the cell homogenates. Protein assays were performed by the method of Lowry *et al.* [25].

### 2.4. Preparation of plasma membranes and western analysis

Plasma membranes were prepared by differential centrifugation and purification on discontinuous sucrose gradients [20]. Membrane proteins were electrophoresed on 7.5% gels in the presence of SDS [26] and electroblotted onto PVDF membranes (DuPont) [27] for detection with protein A-purified GST-hRFC antibody [20] and enhanced chemiluminescence (Pierce). Light emission was recorded on x-ray film with various exposure times, and the signal was quantitated with a computing densitometer and ImageQuant software (Molecular Dynamics).

### 2.5. Southern and northern analysis

Genomic DNAs were isolated from cultured cells using the Puregene DNA isolation kit from Gentra Biosystems, Inc. Aliquots (10  $\mu$ g) were digested with restriction enzymes (*Sac*I or *Hind*III), fractionated on a 0.6% agarose gel, and blotted onto a nylon membrane (Genescreen Plus, DuPont) for Southern hybridization using standard protocols [28]. Total RNA was isolated from log phase cells using the TRIzol Reagent (Life Technologies, Inc./BRL). RNA samples were analyzed on a 0.7% formaldehyde-agarose gel, as previously described [10]. Equal loading was established by staining with ethidium bromide. All membranes were hybridized with  $^{32}$ P-labeled full-length hRFC cDNA and processed as previously described [10]. For Southern analysis, equal loading was confirmed by probing with  $^{32}$ P-labeled cDNA to human FPGS [29].

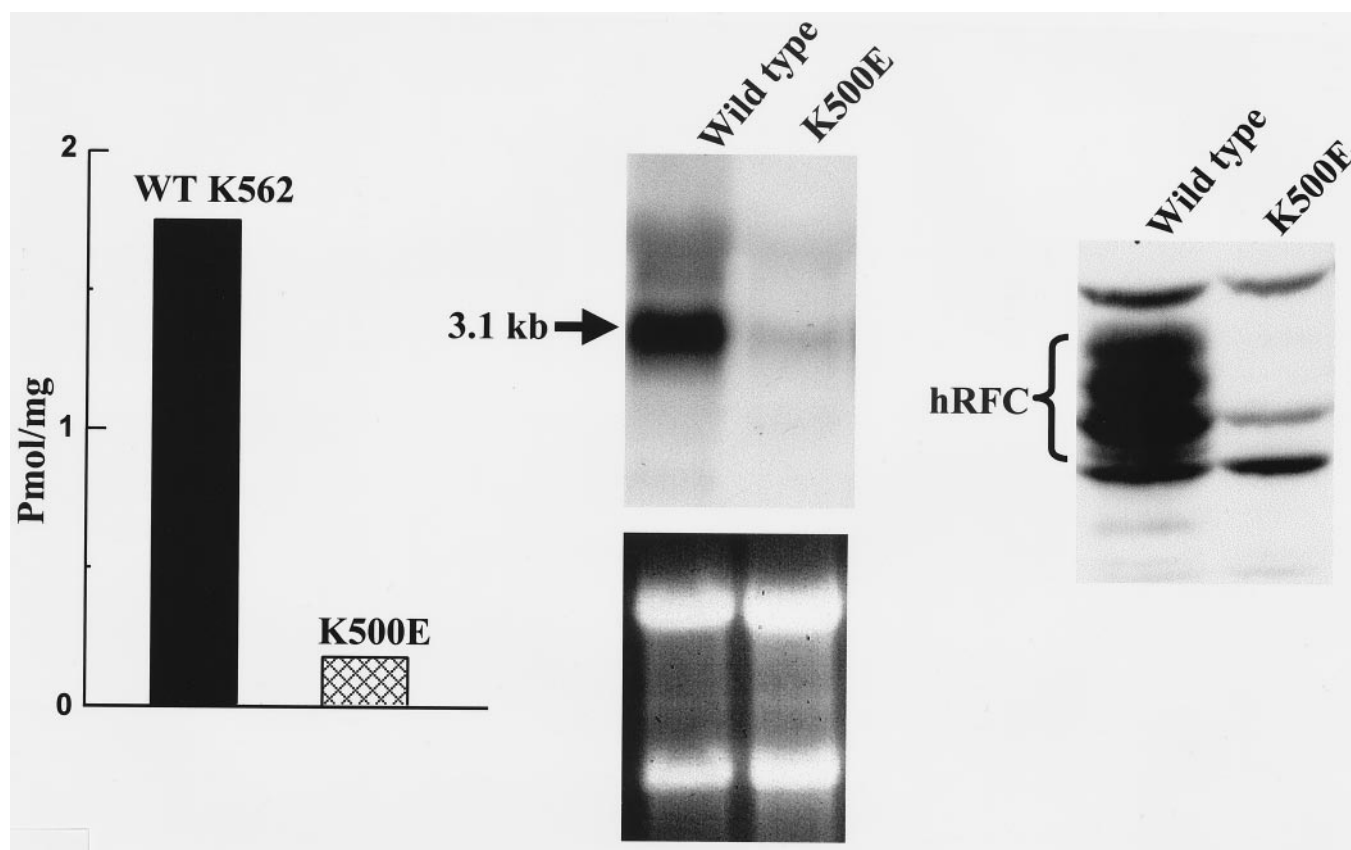


Fig. 1. hRFC transport, hRFC transcripts, and hRFC protein in wild-type K562 and K500E cells. Left panel: Initial rates of [ $^3$ H]MTX uptake were assayed in Hanks' balanced salts medium over 180 sec using  $1 \times 10^7$  cells/mL and 0.5  $\mu$ M MTX. The levels of intracellular radioactive drug were expressed as picomoles per milligram of protein, calculated from direct measurements of radioactivity and protein contents of the cell homogenates. Middle panel: Total RNAs (20  $\mu$ g) were fractionated on a formaldehyde-agarose gel for northern blotting. Equal loading was established by ethidium bromide staining of 28S and 18S RNA (lower). All membranes were hybridized with  $^{32}$ P-labeled full-length hRFC cDNA. Right panel: Membrane proteins (100  $\mu$ g) from wild-type K562 and K500E cells were fractionated on a 7.5% polyacrylamide gel and electroblotted onto a PVDF membrane. Immunoreactive hRFC protein was detected with antibody prepared in rabbits to a GST-hRFC fusion protein [10] and with an enhanced chemiluminescence kit. As previously described [22], hRFC migrates as a broadly banding species centered at  $\sim$ 85 kDa.

## 2.6. Analysis of hRFC transcripts by the 5' rapid amplification of cDNA ends (5'RACE) assay

Double-stranded cDNA with a 5' Marathon cDNA adaptor was synthesized from K562 and K500E poly(A $^+$ ) RNAs using a Marathon cDNA Amplification Kit (Clontech), as recommended by the supplier [30]. Primary PCR and nested PCR reactions were performed using adaptor-ligated cDNA as template and gene-specific RFCo-1 (5'-GCCATGAAGC-CGTAGAAGCAAAGGTAGCACAC) and RFCn-1 (5'-AGCTCCGGAGGGGACGAAGGTGACACTGTG) primers and commercial AP1/AP2 adaptor primers. Primary PCR was carried out for 7 cycles (94 $^\circ$  for 2 sec, 72 $^\circ$  for 3 min) and 36 cycles (94 $^\circ$  for 2 sec, 67 $^\circ$  for 3 min) with the gene-specific RFCo-1 primer and the AP1 adaptor primer using a Perkin-Elmer 9600 DNA Thermal Cycler. Nested PCR on the primary PCR products was carried out for 5 cycles (94 $^\circ$  for 2 sec, 72 $^\circ$  for 3 min) and 20 cycles (94 $^\circ$  for 2 sec, 67 $^\circ$  for 3 min) with the nested gene-specific RFCn-1 and AP2 adaptor primers. 5'-RACE products were subcloned in pGEM-T Easy vector (Promega), and multiple clones were manually sequenced with Sequenase

2.0 (Amersham/U.S. Biochemical Corp.) and [ $\alpha$ - $^{35}$ S-thiol-]dATP.

For analysis of 5'-UTRs (KS6, KS32, KS43; [10, 30]) by RT-PCR, cDNAs were synthesized from total RNA (Perkin-Elmer RT-PCR kit), and amplified with Taq polymerase (Promega) in the presence of GC-rich reagent (Roche) using specific 5'-UTR primers and compatible coding sequence primers. Primer pairs for each hRFC 5'-UTR were based on the DNA sequence for the 5'-untranslated hRFC exons [10, 30] and are as follows (for each pair, listed as sense, antisense): KS6, 5'-CGGGGCCCTGGGGTGAGT, 5'-GCCATGGTGACGCTGTAGAA; KS32-1, 5'-TCTG-GAGGAAAGCGTGGAT, 5'-TGAAGCCGTAGAAGCA-AAGGTA; KS32-2, 5'-GCAATCCCGAGGCGTCTCAG, 5'-CCAGCACGGCCAGGTAGGAGTA; KS32-3, 5'-CT-GTCCATCGGAAACTCCTGTC, 5'-GCCATGGTGACGC-TGTAGAA; KS43, 5'-CGAGTCGCAGGCACAGTGTCAC, 5'-CCAGCACGGCCAGGTAGGAGTA. Three separate KS32 primers (designated KS32/1–3) were employed to identify the different putative splice forms (KS32 I, II, and III) of this 5'-UTR, as previously described [30]. To assess

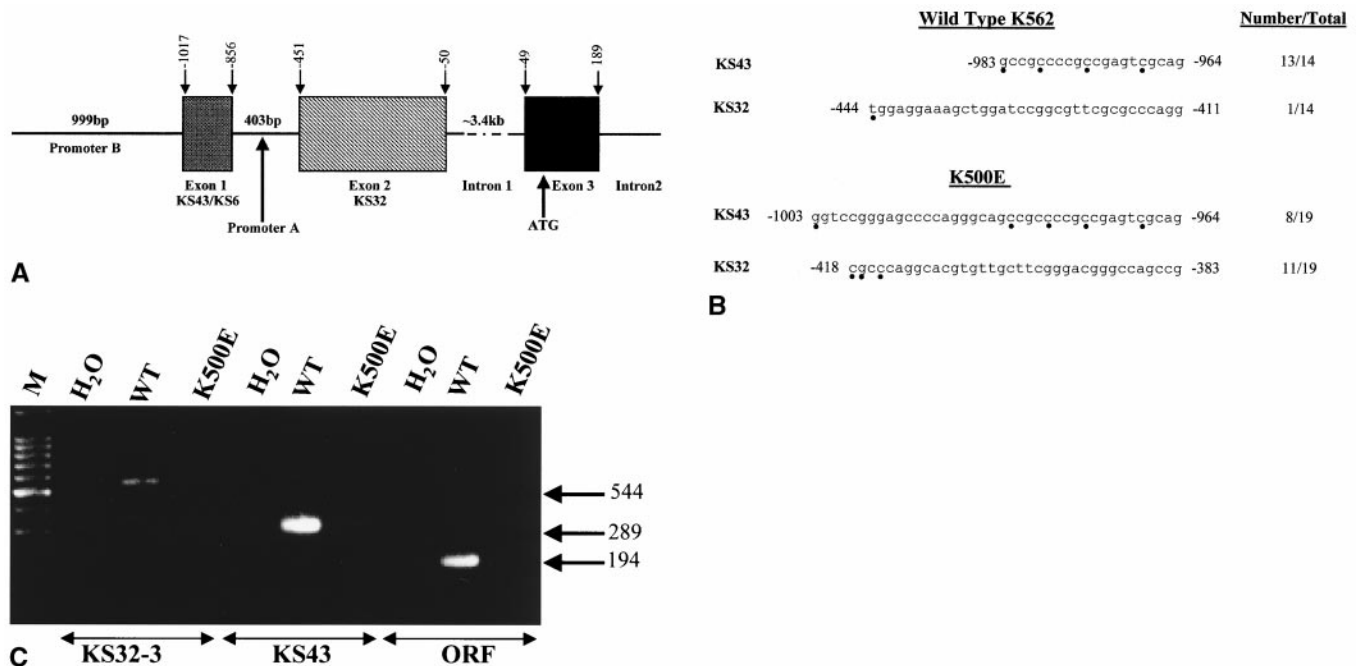


Fig. 2. 5'-RACE and RT-PCR analysis of wild-type K562 and K500E cells. Panel A depicts a schematic of the organization of the upstream region of the hRFC gene including structures of exon 1 (KS43/KS6), exon 2 (KS32), and their respective (designated B and A, respectively) promoters, based on earlier reports [30, 32, 35]. The probable exon junctions are noted. The numbering is for non-intron sequence and is relative to the ATG translational start site. Panel B: Double-stranded cDNA with a 5' Marathon cDNA adaptor was synthesized from poly(A<sup>+</sup>) RNA with a Marathon cDNA Amplification Kit. Primary PCR and nested PCR were performed with adaptor-ligated cDNA as template and gene-specific RFCn-1/RFCn-1 primers and AP1/AP2 adaptor primers [30]. 5'-RACE products were subcloned and sequenced. Sequence data are shown for two separate groups of 5'-RACE products, including KS43 and the alternatively spliced KS32 products [10, 30]. The number is based on the genomic sequence described above. The multiple transcriptional start sites deduced from the 5' ends of the 5'-RACE clones are noted by λ. Both the unique KS43 and KS32 exon fragments shown are fused to a common exon 3 sequence (sequence not shown) starting at position -49 [10, 30]. The number of KS43/KS32 5'-UTR clones and total clones analyzed (i.e. Number/Total) are indicated. Panel C: Total RNA extracted from K562 and K500E cells was used for cDNA synthesis. Template-specific primers for the hRFC KS6, KS32 (3 sets, designated 1–3), and KS43 5'-UTRs, and the hRFC open reading frame (ORF) sequences were used in PCR, as described in "Materials and methods." PCR products were fractionated on a 2% agarose gel and stained with ethidium bromide. Data are shown for a negative control in which water was substituted for cDNA (labeled H<sub>2</sub>O), and for cDNAs amplified from wild-type K562 (labeled WT) and K500E cells. A 100 bp DNA ladder (M) and the sizes of the PCR products are indicated. For the KS32 5'-UTR, only data for the KS32-3 primer set are shown.

the relative levels of hRFC expression, a 194 bp fragment of the hRFC open reading frame (positions -46 to 148) was amplified with RFC-P8 (see above) and RFC/JW1 (5'-GGGTGATGAAGCTCTCCCCTGG). For all primer sets, PCR conditions were: 1 cycle (95° for 4 min) and 30 cycles (95° for 30 sec, 63° for 30 sec, 72° for 45 sec). PCR products were separated on a 2% agarose gel and detected with ethidium bromide staining. In control experiments, all primer sets were found to amplify from purified cDNA templates with similar efficiencies (not shown).

## 2.7. Reporter gene assays of hRFC promoter activities

Reporter gene constructs, including the full-length ("Pro43"; -2016 to -957) and basal (-1088 to -1043; numbering based on non-intron sequence relative to coding sequence ATG start site) hRFC-B promoters [30–32], were cloned in the sense and antisense orientations in pGL3-Basic vector (Promega). Plasmid constructs were isolated with Wizard Midi Prep plasmid isolation kits (Promega) for transient transfections. hRFC-luciferase fusion gene con-

structs or pGL3-Promoter or -Basic control vectors (2.5 μg) were co-transfected with 0.1 μg of pRL-SV40 plasmid (Promega) into logarithmically growing K562 and K500E cells using Lipofectin (Life Technologies), as recommended by the manufacturer. Lipofectin treatments were for ~20 hr and, after an additional 48 hr of incubation in complete RPMI 1640/20% iron-supplemented calf serum, cells were harvested and lysates were prepared. Firefly luciferase activities were assayed with a Dual-Luciferase Reporter Assay System (Promega) in a Turner TD2420 luminometer and normalized to Renilla luciferase activity, as previously described [30].

## 2.8. Sequence analysis of hRFC gene and upstream 5'-flanking region

hRFC cDNAs were synthesized from total RNA with random hexamers using Superscript reverse transcriptase (Life Technologies). The RFC-P8 (5'-CAGTGTCACCTTCGTCCCCCTCCG) and RFC-P10 (5'-CACCCACCTCTTCCAGCAACAAA) primers and Advantage Tth Polymerase mixture (Clontech) were used to amplify the entire



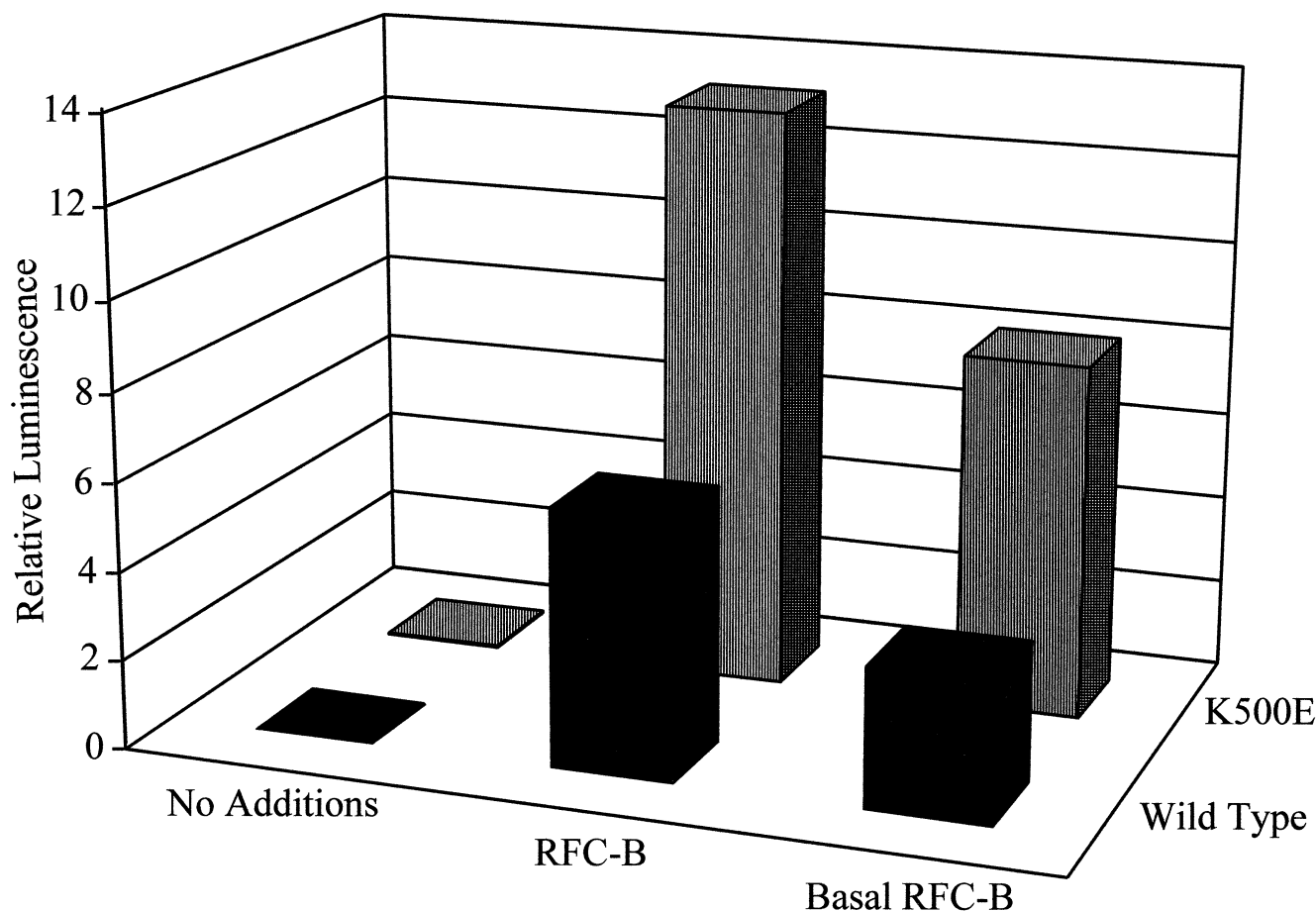


Fig. 3. Reporter gene assays of hRFC-B promoter activities in wild-type K562 and K500E cells. hRFC promoter-reporter gene constructs (2.5  $\mu$ g), including the full-length sense (positions –2016 to –957; labeled “RFC-B”) and the basal (–1088 to –1043) promoters in the pGL3-Basic vector (Promega), were transfected with 0.1  $\mu$ g of pRL-SV40 (Promega) into logarithmically growing wild-type K562 and K500E cells. Lipofectin treatments were for 20 hr, and, after an additional 48 hr of incubation, cells were harvested and lysates were prepared. Firefly luciferase activities were normalized to *Renilla* luciferase activity. The results shown are the mean values for 3–4 experiments. Standard error values were less than 10%.

(~1.8 kb) hRFC coding region. PCR conditions were 94° for 30 sec, 63° for 45 sec, and 72° for 1 min (35 cycles), ending with 72° for 7 min (1 cycle). PCR products were subcloned into the pGEM-T Easy vector (Promega), and the nucleotide sequences were determined by dideoxynucleotide sequencing of three separate cDNA clones with the Sp6 and T7 primers, and with four overlapping gene-specific primers.

The upstream hRFC genomic sequence from positions –50 to –3978 [numbers corresponding to the non-intron genomic sequence where the first base (A) of the putative coding sequence start is +1] was PCR amplified as ~500–1500 bp fragments with Taq and GC-rich reagent (Roche), using gene-specific primers. Primer design was based on our published hRFC upstream gene sequence [30, 32] through position –2016 and from additional upstream sequence, determined from a genomic clone isolated from an EMBL3 Sp6/T7 human peripheral blood leukocyte genomic library (Clontech; [32]). Replicate PCR products were subcloned into pGEM-T Easy plasmid (Promega) for sequencing with

universal primers, or sequenced directly, by automated sequencing with gene-specific primers.

#### 2.9. Analysis of wild-type K562 and K500E cells by SKY analysis and FISH

Cultured cells were treated with colcemid for 2 hr, and mitotic cells were harvested. Chromosomal slides were prepared using standard protocols, which included hypotonic treatment, fixation, and air drying [33]. After treatment with pepsin and fixation with formaldehyde, the chromosome preparations were dehydrated, denatured, and hybridized with painting probes (SkyPaint) for ~48 hr at 37°. The slides were washed, and the chromosomes were stained with DAPI and mounted with an antifading agent. For both the spectral and DAPI images, 10–20 mitotic figures with high quality hybridization signals (minimal overlap) were captured with a CCD camera. Chromosomes were karyotyped according to the color and size of each chromosome, using software developed by Applied Spectral Imaging.

For FISH analysis, both a 17 kb genomic fragment of the

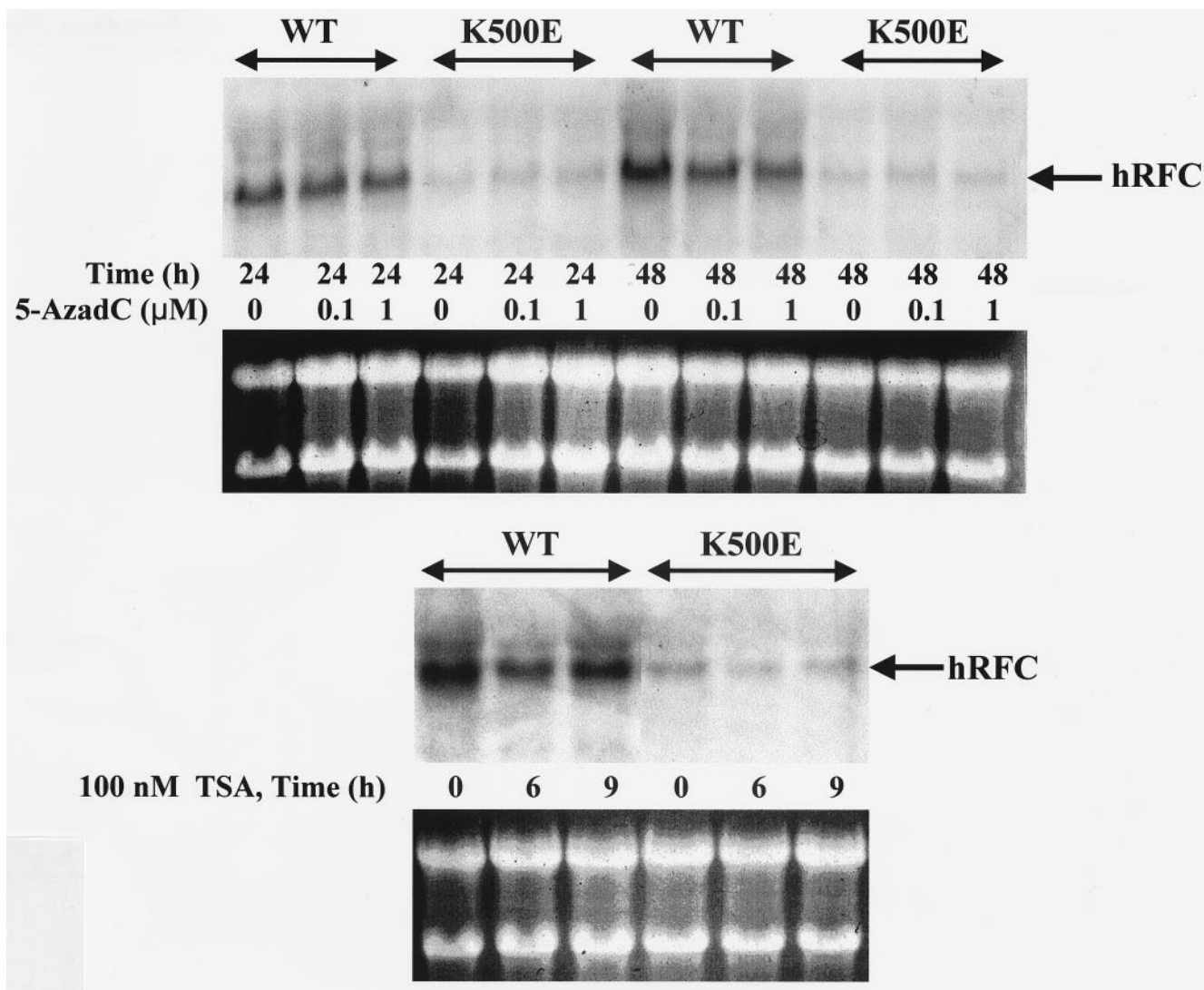


Fig. 4. Effects of 5-aza-2'-deoxycytidine and trichostatin A on hRFC transcripts in wild-type (WT) K562 and K500E cells. Upper panel: Cells in culture were treated with 5-aza-2'-deoxycytidine (5-AzadC; 0,  $10^{-8}$ ,  $10^{-7}$ , and  $10^{-6}$  M) for 24 and 48 hr. Lower panel: Cells were treated with trichostatin A (TSA; 100 nM, 6 and 9 hr). Total RNAs were prepared and analyzed on northern blots, as described for Fig. 1. For each blot, ethidium-stained 18S and 28S RNAs are shown to normalize for loading.

hRFC gene (RFC-g1), isolated from a leukocyte genomic library [30, 32] and directly labeled with Spectrum Green dUTP (Vysis), and a 21q22.2 Spectrum Orange (Vysis) probe were used. Slides were hybridized for 120 hr, washed, and counterstained with DAPI. Images were acquired and digitized with a fluorescence microscope/CCD camera interfaced to a computer workstation.

### 3. Results and discussion

#### 3.1. Association of impaired MTX transport in K500E cells with exceedingly low levels of hRFC transcripts and immunoreactive hRFC protein

The MTX-resistant K500E erythroleukemia subline (157x resistance) was originally isolated in this labora-

tory from wild-type K562 cells by clonal selection in 500 nM MTX [22]. Upon characterization of this resistant phenotype, a number of biochemical alterations were described including increased levels of DHFR (7.7-fold), decreased thymidylate synthase (58%), and severely impaired ( $\sim 90\%$ ) MTX membrane transport by hRFC (Fig. 1, left panel; [22]). On northern blots, there was a nearly complete loss of the major 3.1 kb hRFC transcript (Fig. 1, middle panel) and undetectable hRFC protein on western blots probed with GST-hRFC antibody (Fig. 1, right panel). Likewise, no hRFC protein was detected in K500E cells by photoaffinity labeling with APA- $^{125}$ I-ASA-Lys [22]. Although the low signal on northern blots precludes accurate determinations of transcript levels, by competitive RT-PCR, this has been determined to be 10% of wild-type levels [7]. Thus, K500E cells represent

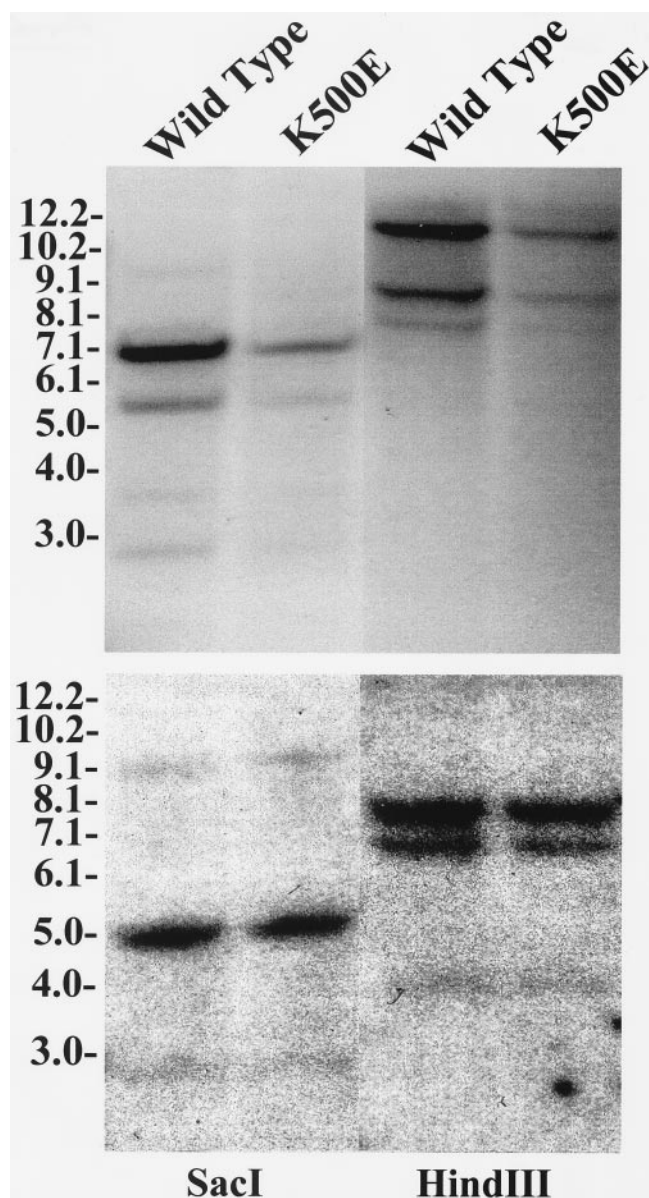


Fig. 5. Association of loss of hRFC activity with loss of hRFC gene copies by Southern blotting. Genomic DNAs (10  $\mu$ g) from wild-type K562 and K500E cells were digested with *SacI* and *HindIII*, fractionated on a 0.6% agarose gel, and blotted onto a nylon membrane (Genescreen Plus). The membrane was hybridized with  $^{32}$ P-labeled full-length hRFC cDNA (upper panel) or FPGS (lower panel).

an excellent hRFC-null human background for expression of the exogenous hRFC gene [20,22,34].

### 3.2. 5'-RACE and RT-PCR analysis of hRFC 5'-UTRs and hRFC promoter utilization

Our previous studies of the 5'-upstream region of the hRFC gene [30] confirmed the presence of 5'-UTR heterogeneity resulting from multiple transcriptional starts and variable splicing of two alternative non-coding exons (designated exons 1 and 2, for the KS43 and KS32 5'-UTRs,

respectively; see schematic in Fig. 2, panel A), transcribed from separate promoters (designated B and A or, previously, "Pro43" and "Pro32," respectively; [30]). 5'-RACE analysis was used to identify the 5'-hRFC transcript termini in wild-type and K500E cells in order to establish the relative contributions of the B and A hRFC promoters to total hRFC transcriptional activity.

Double-stranded cDNA templates were prepared from wild-type and K500E poly(A<sup>+</sup>) RNAs and ligated to anchor adaptors. After PCR amplification with nested anchor (AP1/AP2) primers and two gene-specific (RFCo-1 and RFCn-1) primers, the 5'-RACE products were ligated into the pGEM-T Easy plasmid for transformation and sequencing. By sequencing fourteen clones amplified from wild-type cDNAs, we identified thirteen clones (92.9%) with sequences identical to that previously described for the KS43 5'-UTR (exon 1) and only a single 5'-RACE clone (7.1%) containing a 33 bp KS32 5'-UTR originating from the 5' end of exon 2 (Fig. 2, panel B). None of the 5'-UTR, previously designated KS6 (positions -942 to -856) and also localized to exon 1 [30, 32, 35], was detected. The variable lengths of the KS43 5'-RACE clones by our analysis likely reflect multiple transcriptional starts, as previously reported [30].

A very different distribution of 5'-UTRs was observed for the residual hRFC transcripts in K500E cells. Of the nineteen 5'-RACE clones sequenced, only eight, or 42.1%, were found to contain the KS43 5'-UTR sequence (Fig. 2, panel B). Rather, the majority (eleven of nineteen or 57.9%) of K500E 5'-RACE clones contained a sequence identical to the KS32 5'-UTR and originated from exon 2 [30, 32, 35]. Using an estimate of 10% of total wild-type hRFC transcripts (both KS43 and KS32 UTRs; [7]) in K500E cells, this gives a value of 4.53% (4.2/92.9) of wild-type levels of KS43 transcripts transcribed from the hRFC-B promoter. For the KS32 hRFC transcripts, the levels are essentially unchanged (5.8/7.1 or 81.8%) from the wild type.

In contrast to our previous results with CCRF-CEM cells [30], all of the KS32 transcripts in the K500E/K562 sublines appeared to be splice forms containing only the most 5'-UTR sequence (designated "KS32II" in Ref. 30; positions -444 to -411 and from -418 to -383, respectively; Fig. 2, panel B).

For both wild-type and K500E cells, analogous results were obtained by PCR amplification of the KS6/KS32/KS43 5'-UTRs using primers specific to the unique hRFC non-coding exons and to the downstream hRFC coding sequence (Fig. 2, panel C). Although three separate primer sets were used to identify potential splice forms for the KS32 5'-UTRs [30], KS32 transcripts were generally undetectable (in Fig. 2, panel C, a very light band was detectable from the wild-type cells with the KS32-3 primer set). These data corroborate the 5'-RACE results and further indicate that the dramatically decreased levels of hRFC transcripts in the MTX-resistant K500E subline result primarily from a



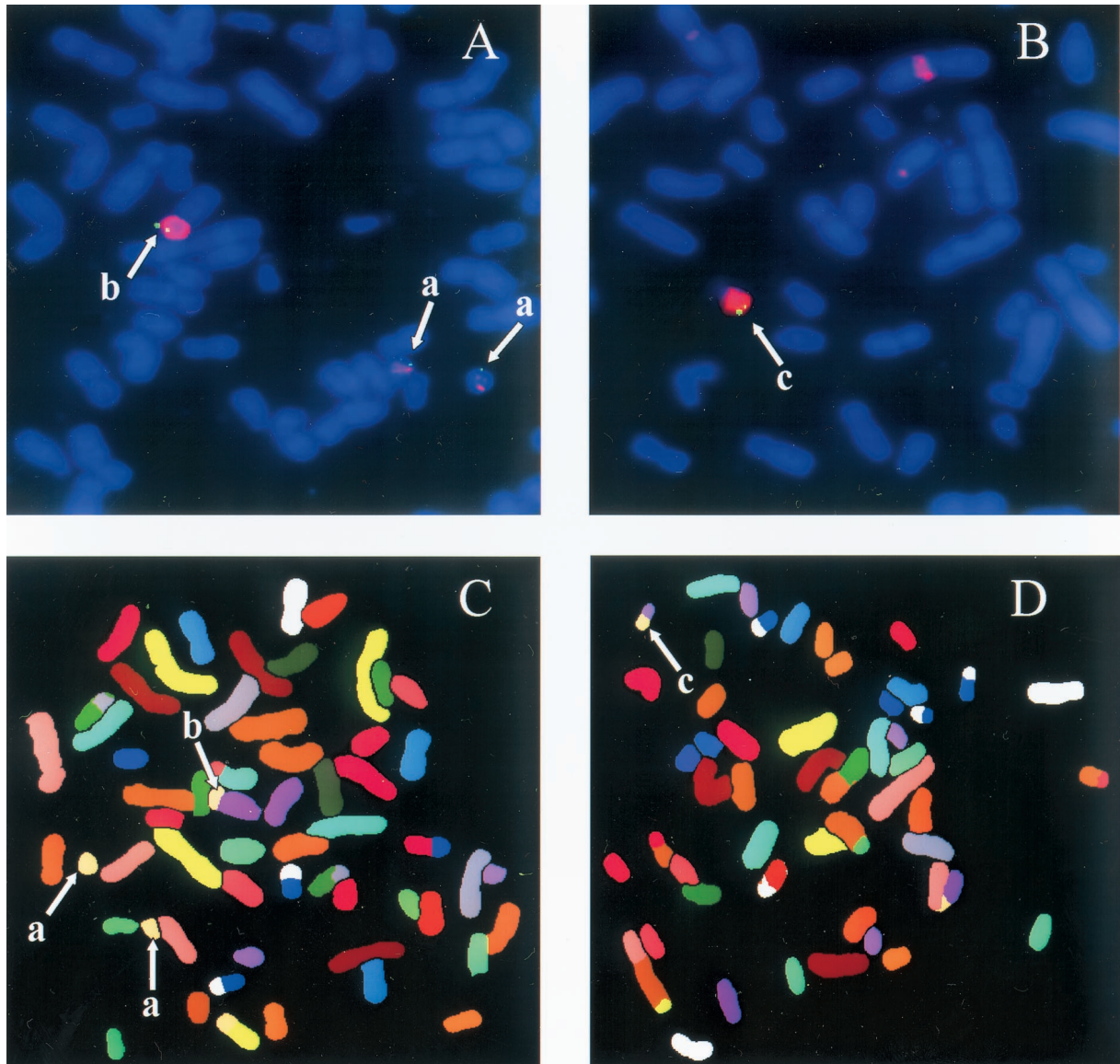


Fig. 6. FISH and SKY analyses of wild-type K562 (panels A and C) and K500E (panels B and D) cells. (A and B) A combination of a commercial 21q22 probe (labeled with Spectrum Orange) and a hRFC genomic probe (RFC-g1, 17 kb; in EMBL2 SP6/T7; labeled with Spectrum Green) was used to probe metaphase spreads from wild-type K562 and K500E cells. In wild-type cells (total of 83 metaphases), up to 6 chromosomes showed a 21q22 signal (panel A). Two of these were identical to normal copies of chromosome 21 (labeled *a*) and showed an hRFC signal at the q terminal region (at 21q22.2). There were 2–4 hRFC signals per wild-type metaphase, including those associated with 1–2 medium subtelocentric chromosomes (labeled *b*). For K500E cells (panel B), the only consistent hRFC signal detected in 47 metaphases involved a small metacentric chromosome (labeled *c*), representing a fusion between chromosomes 21 and 22. An additional large metacentric chromosome of unknown origin was identified in the majority of metaphases, which hybridized to the 21q22 probe without hRFC. (panels C and D) SKY analysis of wild-type K562 (left panel) and K500E cells (right panel) showing normal copies of chromosome 21 (labeled *a*), a 12;21 fusion chromosome (labeled *b*), and, for K500E cells, a 21;22 fusion chromosome (labeled *c*).

decrease of KS43 transcripts containing non-coding exon 1, which is under control of the hRFC-B promoter.

### 3.3. Reporter gene assays of the hRFC promoters

The apparent decrease in activity of the upstream hRFC-B promoter in K500E compared with wild-type cells may reflect differences in the intracellular levels or compositions of critical transcription factors. To explore this possibility, luciferase reporter gene constructs (in pGL3 basic)

containing the full length (–2016 to –957) or 46 bp basal (–1088 to –1043) hRFC-B promoters [30, 31] were transiently expressed in K500E and wild-type K562 cells. Firefly luciferase activities were assayed and normalized to *Renilla* luciferase activity, encoded by a cotransfected pRL-SV40 plasmid. For both cell lines, the sense hRFC-B promoter constructs resulted in luciferase activities far in excess of the promoterless pGL3-basic construct (Fig. 3), or constructs in which the hRFC-B promoter fragments were ligated in antisense orientations (not shown).



Despite the exceedingly low levels of total and KS43 hRFC transcripts in K500E cells (Figs. 1 and 2), promoter activities were high for both basal and full-length hRFC-B constructs. Indeed, luciferase activity was actually *increased* (3- and 2-fold, respectively, for the basal and full-length constructs) in K500E cells over the levels measured in wild-type cells (Fig. 3).

Thus, the results of our reporter gene assays are clearly not reflective of the dramatic losses of hRFC transcripts in K500E cells. Moreover, they strongly suggest that neither differences in intracellular concentrations nor compositions of critical transcription factors between the drug-resistant and -sensitive sublines are likely to account for their disparate levels of hRFC expression.

### 3.4. Effects of 5-aza-2'-deoxycytidine and trichostatin A on hRFC transcripts

The decrease in hRFC transcripts in K500E cells could reflect the loss of hRFC transcriptional activity. This could arise from differences in methylation of CpG dinucleotides [36] in the GC-rich (87%) hRFC-B promoter or from deacetylation of core histones [37]. To assess these possibilities, K500E and wild-type cells were treated with the demethylating agent 5-aza-2'-deoxycytidine (0.1 or 1  $\mu$ M; 24–48 hr), or the histone deacetylase inhibitor trichostatin A (100 nM, 6 and 9 hr) [38]. Neither treatment resulted in any noticeable change in the levels of hRFC transcripts in either cell line (Fig. 4). Therefore, the low levels of hRFC transcripts in K500E cells are not likely to result from changes in hRFC-B promoter methylation or from transcription repression due to deacetylation of core histones.

### 3.5. Structural alterations involving the hRFC gene locus in K500E cells

When genomic DNAs from wild-type and K500E cells were restriction digested (*Sac*I, *Hind*III) and analyzed on Southern blots probed with full-length KS43 hRFC cDNA [10], there were no differences between the lines in overall hRFC gene structure, as reflected in the patterns of hybridizing restriction fragments (Fig. 5, upper panel). However, the *intensities* of the hRFC bands for the K500E cells were noticeably lower and approximated 42.20% ( $\pm$  6.63%, SEM; N = 4) of the value for wild-type cells (Fig. 5). When the same blot was stripped and rehybridized to cDNA for human FPGS, there were no significant differences in the intensities of the hybridizing bands (Fig. 5, lower panel). Although there is no evidence for structural alterations within the hRFC gene locus itself, our Southern analysis strongly suggests that the markedly decreased levels of hRFC transcripts in K500E cells, in part, result from the loss of one or more hRFC alleles.

No DNA sequence differences in the 5'-UTRs or hRFC coding region were observed between the cell lines following 5'-RACE (see above) or RT-PCR, and sequencing of

the PCR-amplified products (data not shown). Upstream sequences, including all of exon 2 (e.g. KS32, starting at position –50), both of the hRFC-A and -B promoters, and additional flanking sequence up to position –3978, were PCR amplified from both K562 and K500E genomic DNAs. Once again, upon sequencing the PCR products from multiple amplifications, there were no reproducible sequence differences between the lines. Thus, although the K500E subline is characterized by an apparent loss of hRFC gene copies, the residual hRFC gene, including both the RFC-B and -A promoters, is completely intact.

### 3.6. SKY and FISH analyses of wild-type K562 and K500E cells

SKY and FISH analyses of the hRFC gene were performed to clarify the molecular bases for the loss of greater than 50% of the hRFC signal on Southern blots of K500E genomic DNA, and to explore the possibility that chromosomal translocations including the hRFC gene locus may be associated with the transport-impaired phenotype. For FISH analysis, both hRFC genomic (Spectrum Green-labeled) and 21q22-specific (Spectrum Orange-labeled) probes were used (Fig. 6).

In wild-type cells (total of 83 metaphases), up to 6 chromosomes showed a 21q22 signal (Fig. 6A), 2 of which were identical to normal copies of chromosome 21 (labeled *a*) and showed an hRFC signal at the q terminal region (at 21q22.2), as previously described [11]. In addition, hRFC and 21q22 labeling was consistently detected in 1–2 medium subtelocentric chromosomes (an example is labeled *b* in Fig. 6A). Altogether, there were three, and occasionally four, hRFC signals per wild-type metaphase. By SKY analysis, two normal copies of chromosome 21 (labeled *a*) and a 12;21 fusion chromosome (labeled *b*, in Fig. 6C) were detected in wild-type K562 cells.

For K500E cells, no normal copies of chromosome 21 were detected. Rather, the only consistent hRFC signal detected in 47 metaphases involved a single small metacentric chromosome (labeled *c* in Fig. 6B), confirmed by SKY analysis to be a fusion between chromosomes 21 and 22 (labeled *c* in Fig. 6D). Other translocations involving chromosome 21 were detected in K500E by SKY. These include 12;21 and 1;21; however, from FISH, these did *not* appear to involve the hRFC gene locus. For instance, in panel B, a large (unidentified) metacentric chromosome was found to hybridize to the 21q22 probe without hRFC.

## 4. Conclusion

In conclusion, the mechanistic bases for the nearly complete loss of hRFC transcripts and immunoreactive hRFC protein in the transport-impaired K562 subline, K500E, were characterized. Losses of hRFC transcripts were selective for those containing exon 1 (KS43) non-coding se-

quence and transcribed from the upstream hRFC-B promoter. Paradoxically, hRFC-B activity in K500E cells was uniquely high in transient reporter gene assays with exogenous promoter constructs. This implies that differences in the levels of critical transcription factors between the lines were not causal in their disparate hRFC expressions. Likewise, through the use of specific inhibitors (5-aza-2'-deoxycytidine and trichostatin A), we were able to exclude potential transcriptional repressive roles of promoter methylation and histone deacetylation in the K500E phenotype. No sequence differences between K500E and wild-type cells were detectable in the hRFC coding region and in nearly 4 kb of upstream sequence, including the non-coding exons 1 and 2 and the hRFC-A and -B promoters. However, this lack of change is offset by our finding of a complete loss of a majority (1 to 3) of hRFC alleles in wild-type K562 cells and a translocation of the sole remaining hRFC allele to chromosome 22. The significant differential between the nearly complete loss of hRFC transcripts and the loss of transcripts directly attributable to decreased numbers of hRFC alleles (~60%, from Southern analysis) is presently unexplained, but may involve transcriptional silencing resulting from the 21;22 chromosomal translocation, including the hRFC gene.

## Acknowledgments

This work was supported by NIH Grant CA53535.

## References

- [1] Chu E, Allegra CJ. Antifolates. In: Chabner BA, Longo DL, editors. Cancer chemotherapy and biotherapy: principles and practice. 2nd ed. Philadelphia: Lippincott-Raven, 1996. p. 109–48.
- [2] Goldman ID, Matherly LH. The cellular pharmacology of methotrexate. *Pharmacol Ther* 1985;28:77–102.
- [3] Sirotinak FM. Obligate genetic expression in tumor cells of a feta membrane property mediating “folate” transport: biological significance and implications for improved therapy of human cancer. *Cancer Res* 1985;45:3992–4000.
- [4] Schuetz JD, Matherly LH, Westin EH, Goldman ID. Evidence for a functional defect in the translocation of the methotrexate transport carrier in a methotrexate-resistant murine L1210 leukemia cell line. *J Biol Chem* 1988;263:9840–7.
- [5] Sirotinak FM, Moccio DM, Kelleher LE, Goutas LJ. Relative frequency and kinetic properties of transport-defective phenotypes among methotrexate resistant L1210 clonal cell lines derived *in vivo*. *Cancer Res* 1981;41:4442–52.
- [6] Gorlick R, Goker E, Trippett T, Steinherz P, Elisseyeff Y, Mazumdar M, Flintoff WF, Bertino JR. Defective transport is a common mechanism of acquired methotrexate resistance in acute lymphoblastic leukemia and is associated with decreased reduced folate carrier expression. *Blood* 1997;89:1013–8.
- [7] Zhang L, Taub JW, Williamson M, Wong SC, Hukku B, Pullen J, Ravindranath Y, Matherly LH. Reduced folate carrier gene expression in childhood acute lymphoblastic leukemia: relationship to immunophenotype and ploidy. *Clin Cancer Res* 1998;4:2169–77.
- [8] Dixon KH, Lampher BC, Chiu J, Kelley K, Cowan KH. A novel cDNA restores reduced folate carrier activity and methotrexate sensitivity to transport deficient cells. *J Biol Chem* 1994;269:17–20.
- [9] Williams FRM, Murray RC, Underhill TM, Flintoff WF. Isolation of a hamster cDNA clone coding for a function involved in methotrexate uptake. *J Biol Chem* 1994;269:5810–6.
- [10] Wong SC, Proefke SA, Bhushan A, Matherly LH. Isolation of human cDNAs that restore methotrexate sensitivity and reduced folate carrier activity in methotrexate transport-defective Chinese hamster ovary cells. *J Biol Chem* 1995;270:17468–75.
- [11] Moscow JA, Gong M, He R, Sgagias MK, Dixon KH, Anzick SL, Meltzer PS, Cowan KH. Isolation of a gene encoding a human reduced folate carrier (*RFCL*) and analysis of its expression in transport-deficient, methotrexate-resistant human breast cancer cells. *Cancer Res* 1995;55:3790–4.
- [12] Williams FRM, Flintoff WF. Isolation of a human cDNA that complements a mutant hamster cell defective in methotrexate uptake. *J Biol Chem* 1995;270:2987–92.
- [13] Prasad PD, Ramamoorthy S, Leibach FH, Ganapathy V. Molecular cloning of the human placental folate transporter. *Biochem Biophys Res Commun* 1995;206:681–7.
- [14] Brigle KE, Spinella MJ, Sierra EE, Goldman ID. Characterization of a mutation in the reduced folate carrier in a transport defective L1210 murine leukemia cell line. *J Biol Chem* 1995;270:22974–9.
- [15] Roy K, Tolner B, Chiao JH, Sirotinak FM. A single amino acid difference within the folate transporter encoded by the murine RFC-1 gene selectively alters its interaction with folate analogues. Implications for intrinsic antifolate resistance and directional orientation of the transporter within the plasma membrane of tumor cells. *J Biol Chem* 1998;273:2526–31.
- [16] Zhao R, Assaraf YG, Goldman ID. A reduced folate carrier mutation produces substrate-dependent alterations in carrier mobility in murine leukemia cells and methotrexate resistance with conservation of growth in 5-formyltetrahydrofolate. *J Biol Chem* 1998;273:7873–9.
- [17] Zhao R, Assaraf YG, Goldman ID. A mutated murine reduced folate carrier (*RFCL*) with increased affinity for folic acid, decreased affinity for methotrexate, and an obligatory anion requirement for transport function. *J Biol Chem* 1998;273:19065–71.
- [18] Jansen G, Mauritz R, Drori S, Sprecher H, Kathmann I, Bunni M, Priest DG, Noordhuis P, Schornagel JH, Pinedo HM, Peters GJ, Assaraf YG. A structurally altered human reduced folate carrier with increased folic acid transport mediates a novel mechanism of antifolate resistance. *J Biol Chem* 1998;273:30189–98.
- [19] Gong M, Yess J, Connolly T, Ivy SP, Ohnuma T, Cowan KH, Moscow JA. Molecular mechanism of antifolate transport deficiency in a methotrexate resistant MOLT-3 human leukemia cell line. *Blood* 1997;89:2494–9.
- [20] Wong SC, Zhang L, Witt TL, Proefke SA, Bhushan A, Matherly LH. Impaired membrane transport in methotrexate-resistant CCRF-CEM cells involves early translation termination and increased turnover of a mutant reduced folate carrier. *J Biol Chem* 1999;274:10388–94.
- [21] Sadlish H, Murray RC, Williams FRM, Flintoff WF. Mutations in the reduced folate carrier affect protein localization and stability. *Biochem J* 2000;346:509–16.
- [22] Wong SC, McQuade R, Proefke SA, Bhushan A, Matherly LH. Human K562 transfectants expressing high levels of reduced folate carrier but exhibiting low transport activity. *Biochem Pharmacol* 1997;53:199–206.
- [23] Tse A, Brigle K, Taylor SM, Moran RG. Mutations in the reduced folate carrier gene which confer dominant resistance to 5,10-dideazatetrahydrofolate. *J Biol Chem* 1992;273:25953–60.
- [24] Fry DW, Yalowich JC, Goldman ID. Rapid formation of folylpolyglutamyl derivatives of methotrexate and their association with dihydrofolate reductase as assessed by high pressure liquid chromatography in the Ehrlich ascites tumor. *J Biol Chem* 1982;257:1890–6.

- [25] Lowry OH, Rosebrough NJ, Farr AL, Randall RJ. Protein measurement with the Folin phenol reagent. *J Biol Chem* 1951;193:265–75.
- [26] Laemmli UK. Cleavage of structural proteins during the assembly of the head of bacteriophage T4. *Nature* 1970;227:680–5.
- [27] Matsudaira P. Sequence from picomole quantities of proteins electrophoretically transferred onto polyvinylidene difluoride membranes. *J Biol Chem* 1987;262:10035–8.
- [28] Maniatis T, Fritsch EF, Sambrook J. *Molecular cloning: a laboratory manual*. Cold Spring Harbor, New York: Cold Spring Harbor, 1989.
- [29] Garrow TA, Admon A, Shane B. Expression cloning of a human cDNA encoding folylpoly( $\gamma$ -glutamate) synthetase and determination of its primary structure. *Proc Natl Acad Sci USA* 1992;89:9151–5.
- [30] Zhang L, Wong SC, Matherly LH. Transcript heterogeneity of the human reduced folate carrier results from the use of multiple promoters and variable splicing of alternative upstream exons. *Biochem J* 1998;332:773–80.
- [31] Whetstone JR, Matherly LH. The basal promoters for the human reduced folate carrier gene are regulated by a GC-box and a CRE/AP-1-like element: Basis for tissue-specific gene expression. *J. Biol. Chem.*, in press.
- [32] Zhang L, Wong SC, Matherly LH. Structure and organization of the human reduced folate carrier gene. *Biochim Biophys Acta* 1998;1442:389–93.
- [33] Heng HHQ, Tsui LC. Modes of DAPI banding and simultaneous *in situ* hybridization. *Chromosoma* 1993;102:325–32.
- [34] Wong SC, Zhang L, Proefke SA, Matherly LH. Effects of the loss of capacity for N-glycosylation on the transport activity and cellular localization of the human reduced folate carrier. *Biochim Biophys Acta* 1998;1375:6–12.
- [35] Tolner B, Roy K, Sirotinak FM. Structural analysis of the human RFC-1 gene encoding a folate transporter reveals multiple promoters and alternatively spliced transcripts with 5' end heterogeneity. *Gene* 1998;211:331–41.
- [36] Singal R, Ginder GD. DNA methylation. *Blood* 1999;93:4059–70.
- [37] Pazin MJ, Kadonaga JT. What's up and down with histone deacetylation and transcription? *Cell* 1997;89:325–8.
- [38] Yoshida M, Kijimima M, Akita M, Beppu T. Potent and specific inhibition of histone deacetylase both *in vitro* and *in vivo* by trichostatin A. *J Biol Chem* 1990;265:17174–9.